Mechanistic acute-to-chronic extrapolation through sediment toxicokinetic-toxicodynamic modeling

Journal:	*Environmental Science & Technology*
Manuscript ID	es-2025-13691h
Manuscript Type:	Article
Date Submitted by the Author:	28-Sep-2025
Complete List of Authors:	Xiao, Wenze; Xiamen University, College of the Environment and Ecology Simpson, Stuart; CSIRO Environment Business Unit, Industry Environments Tan, Qiao-Guo; Xiamen University, College of the Environment and Ecology Xie, Minwei; Xiamen University, College of the Environment and Ecology

Mechanistic acute-to-chronic extrapolation through sediment toxicokinetic-toxicodynamic modeling

Wenze Xiao[1], Stuart L. Simpson[2], Qiao-Guo Tan[1], Minwei Xie[1*]

1. Fujian Provincial Key Laboratory for Coastal Ecology and Environmental Studies, State Key Laboratory of Marine Environmental Science, Key Laboratory of the Ministry of Education for Coastal and Wetland Ecosystem, College of the Environment and Ecology, Xiamen University, Xiamen, Fujian, 361102, China

2. CSIRO Environment, Ecosciences Precinct, 41 Boggo Road, QLD 4102, Australia

*Corresponding Author: minweixie@xmu.edu.cn

TOC Graphic

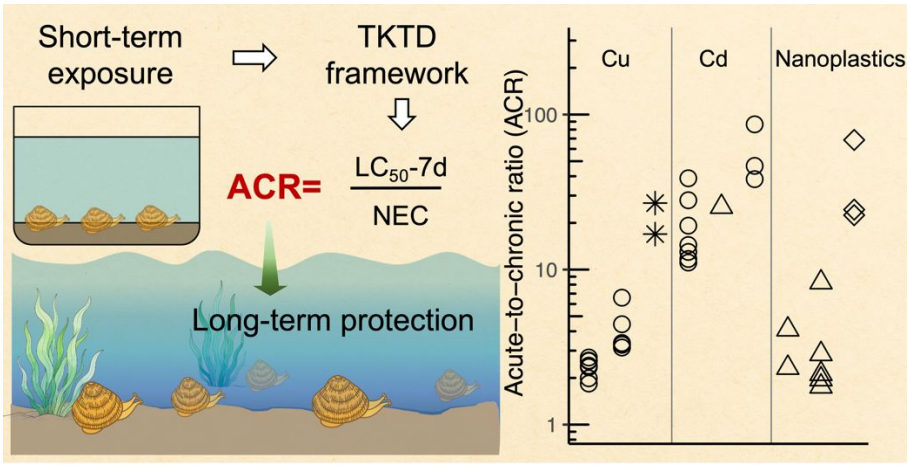

Abstract

Ecological risk assessment often requires extrapolation from short-term laboratory-derived effects data to predict long-term ecological impacts of pollution exposure. This study developed a mechanistic toxicokinetic-toxicodynamic (TKTD) modeling framework to derive acute-to-chronic ratios (ACRs) for the benthic clam *Ruditapes philippinarum* exposed to sediment-associated Cu. To facilitate model development in the sediment context, we derived physiological parameters (k_e, C_{IT}, k_m) using aqueous toxicity tests and used diffusive gradients in thin-films (DGT) measurements to represent Cu bioavailability in sediments. The sediment TKTD model accurately predicted Cu accumulation in clam tissues and adequately predicted toxicity, with a 10% deviation from observed effects. Using model-predicted 7-day LC_{50} and no-effect concentration, an ACR of 17 was determined for Cu-induced clam mortality. The framework was then applied to derive ACRs for other contaminants using literature derived aqueous TKTD parameters, including cadmium (ACR_{Cd}: 11–87) and nanoplastic particles (ACR_{NPs}: 1.9–69)The new approach was also effective for elucidating how environmental variables (e.g., salinity, nanoplastics size) influence ACR values, thus offering insight which may be difficult to achieve by traditional empirical approaches. The study demonstrates the utility of TKTD modeling as a transparent and reproducible mechanistic method for acute-to-chronic extrapolation of toxicity as used for risk assessment applications.

Keywords: TKTD; ACR; extrapolation; ecological risk assessment; *Ruditapes philippinarum*

Synopsis

Using toxicokinetic-toxicodynamic modeling, we derived acute-to-chronic ratios (ACRs) for Cu toxicity necessary to bridge between short-term test data and long-term ecological impact prediction. The kinetic modelling approach also enables environmental factors affecting ARC extrapolation uncertainty to be explored.

1.Introduction

Ecological risk assessment often faces the challenge of setting protective thresholds for long-term exposure, while toxicity data are more frequently obtained from short-term, acute tests.[1–3] To bridge this gap, regulators extrapolate chronic thresholds from acute data based on acute-to-chronic ratios (ACRs) or apply generic assessment safety factors.[4–6] ACRs are often derived empirically by comparing acute and chronic datasets from different studies, often involving mismatched species, endpoints, chemicals, or test conditions.[3,7] In practice, inconsistencies across datasets introduce substantial variability, with reported ACR values differing by more than three orders of magnitude.[8] Consequently, assessment factors are often chosen pragmatically from ACR distribution, but no consensus exists on their appropriate size.[9] For example, the European Centre for Ecotoxicology and Toxicology of Chemicals recommends a general factor of 40,[10] while USEPA suggests 8.3 for cadmium,[11] and other studies have reported both higher and lower values.[9,12,13]

Robust ACRs may be obtained from quantitative observations of both acute and chronic effects for the same species and chemical under consistent conditions.[13] However, such data remain scarce. There is an opportunity for kinetic acute toxicity tests combined with kinetic modeling to provide alternative by generating time-dependent toxicity predictions across both acute and chronic time-scales. One such kinetic model, the toxicokinetic-toxicodynamic (TKTD) model, explicitly links contaminant exposure, accumulation, and effects over time.[14,15] As a mechanistic approach, it is expected to provide a more advanced basis for ACR derivation than empirical extrapolation.

TKTD models have been widely developed in water-based systems, whereas their applications to sediments remain limited.[16] Sediments, however, warrant greater attention because they act as long-term contaminant reservoirs and benthic organisms, being relatively immobile, are exposed chronically.[17] Kinetic modeling sediment toxicity is particularly challenging as benthic invertebrates can accumulate contaminants through multiple pathways, including overlying water, porewater, and

ingested particles.[18] Capturing these processes requires highly parametrized models, and fitting numerous parameters with limited experimental resolution risks overfitting.[16] Further, contaminant bioavailability is influenced by its partitioning behavior and controlled by sediment properties such as pH, redox conditions, organic matter composition, and spatial heterogeneity, all of which vary with environmental dynamics.[19,20] All these complexities have slowed the development of TKTD models in sediments, hindering efforts to mechanistically derive ACRs for benthic exposure.

Focusing on metal contaminants, the diffusive gradients in thin-films (DGT) technique offers a practical tool to address TKTD parameterization challenges concerning metal bioavailability. When deployed in sediments, DGT devices accumulate dissolved and dissociable particulate forms of metals, providing an integrated measure of the labile metal pool.[21,22] This proxy for bioavailable metals has been successfully applied to predict both acute and chronic risks to benthic organisms.[23–25] By simplifying the representation of bioavailable metals while retaining ecological relevance, DGT measurements can support kinetic model construction without the need to fully resolve complex sediment processes.

Building on this foundation, the primary objective of this study was to establish a mechanistic framework for ACR derivation by integrating acute kinetic exposure experiments with TKTD modeling in sediments. Two simplifying assumptions were made to achieve this goal. First, DGT-labile metal was treated as the predominant source of bioavailable metal in sediments. Second, key physiological parameters, including efflux rate constant (k_e), sensitivity to internal metal (C_{IT}), and mortality rate constant (k_m) (refer to Section 2.6), are considered species-specific but not environment-dependent, and can therefore be obtained from water-based experiments.

2. Materials and methods

2.1 Experimental organisms and seawater preparation

Ruditapes philippinarum, a bivalve species widely distributed along Asian coastline, was selected for this study, due to its ecological relevance and widespread use as a bioindicator in environmental monitoring and ecotoxicology.[18,26–28] This

species inhabits sandy or muddy intertidal zones and feeds by filtering particles near the sediment water interface.[26,29]

Clams (1.9–2.6 cm shell length) were collected near Jimei Bridge, Xiamen, China (24°35′15″ N, 118°7′21″ E) and immediately transported to the laboratory. They were acclimated for one week in aerated seawater at 30‰ salinity and 21 ± 1°C, under a 14 h light:10 h dark photoperiod. During acclimation, clams were fed the green algae *Chlorella* sp. daily for an hour (~3 mg per clam).

Seawater (salinity = 32‰) was collected from Yefengzhai, Xiamen, China (24°27′12″ N, 118°10′35″ E). It was filtered through a 0.22 μm mixed cellulose ester membrane, and then diluted with deionized water (18.2 MΩ cm, Millipore) to decrease the salinity to 30‰.

2.2 Sediment collection and Cu amendment

Surface sediments (0–5 cm depth) were collected from Dagang Bay, Quanzhou, China (24°57′26″ N, 118°55′2″ E), transported to the laboratory in sealed zip-lock bags, and stored at room temperature (21 ± 1°C).

Copper (Cu) was chosen as the target contaminant due to its high toxicity,[30] widespread occurrence,[31,32] and high ecological risk in aquatic ecosystem.[33–35] Sediment Cu concentrations along the China coast typically range from <10 mg kg^{-1} to 600 mg kg^{-1}, but can reach over 1000 mg kg^{-1} in severely polluted regions.[36] To simulate environmentally relevant contamination and induce observable biological responses within a short experimental timeframe, sediments were prepared with two Cu levels: 400 mg kg^{-1} (Low-Cu) and 800 mg kg^{-1} (High-Cu) dry weight prepared using an spiking and equilibration method described in the Note S1, Supporting Information (SI).[37]

2.3 Aqueous exposure experiments

All experimental containers were polypropylene, pre-cleaned by overnight soaking in 5% HNO_3, and thoroughly rinsed with reverse osmosis water and deionized water to minimize potential metal contamination.

The physiological parameters used to predict Cu toxicity in sediments were

derived from aqueous toxicokinetic and toxicodynamic experiments. Two aqueous experiments were conducted: (i) depuration following a low-level ^{65}Cu exposure to derive the efflux rate constant k_e (denoted as Aq-Low-Cu treatment), and (ii) a high-Cu exposure (denoted as Aq-High-Cu treatment) to determine the internal Cu threshold (C_{IT}) and mortality rate constant (k_m).

2.3.1 Elimination kinetics following low ^{65}Cu exposure (Aq-Low-Cu)

Clams were pre-exposed in triplicate for 2 days in 1.5 L of seawater containing 5 μg L^{-1} of ^{65}Cu (99.7% purity, ISOFLEX, USA) in a flow-through system, with continuous water renewal at 1.0 mL min^{-1}. No food was supplied during this phase. After exposure, clams were transferred to clean seawater (1.5 L) for a 16-day depuration phase, with daily manual water renewal. Three replicates were set. The clams were fed *Chlorella* sp. for 1 h every two days in separate containers before water renewal.

To monitor ^{65}Cu elimination, clams were sampled eight times during 16 days of depuration (two clams per replicate). Immediately after sampling, clams were immersed in 1 mmol L^{-1} EDTA solution (pH = 8.0) to terminate Cu uptake, and then dissected. The soft tissues were rinsed with 1 mmol L^{-1} EDTA, followed by deionized water to remove loosely bound Cu. Tissues were then stored at –20 °C, freeze-dried, weighed, and digested for isotope-specific Cu analysis.

2.3.2 Toxicodynamic responses under high Cu exposure (Aq-High-Cu)

To evaluate toxicodynamic responses, clams were exposed to 400 μg L^{-1} of Cu in seawater for ~10 days until complete mortality occurred. Experiments were run in triplicate with 20 clams per each: 10 for mortality observation and 10 for short-term Cu accumulation kinetics.

During the first 24 h, ^{65}Cu was used for the exposure solution to trace early-stage uptake ($CuCl_2$ was replaced thereafter). Clams for accumulation analysis were sampled five times during 24 h (two clams per replicate) and at each interval, 3 mL of water from each replicate was filtered (0.45 μm PES membrane), pooled, acidified (HNO_3, pH < 2), and stored for Cu analysis.

The remaining 10 clams per replicate were monitored for mortality every 6–12 h,

with water samples collected at the same time. Dead individuals were promptly removed, dissected, and analyzed for tissue Cu. Control groups showed no mortality, confirming that toxicity was attributable to Cu exposure.

2.4 Sediment exposure experiment

To evaluate Cu bioaccumulation and toxicity from sediments, clams were exposed to Cu-spiked and control sediments for 10 days. Bioavailable Cu at the sediment-water interface was characterized using the DGT technique.

Nine plastic boxes (30 × 9 × 12 cm) served as exposure chambers, assigned to uncontaminated sediment (Sed-control), low-Cu sediment (Sed-Low-Cu treatment), or high-Cu sediment (Sed-High-Cu treatment) (Section 2.2), with three replicates per treatment. Sediment was added to 1 cm depth and overlaid with 10 cm of clean seawater. The sediment-water system was equilibrated undisturbed for 48 h before clam introduction. To reduce Cu accumulation in the overlying water, clean seawater was continuously renewed at a one-day turnover rate, and manual renewal was performed daily to facilitate sampling.

For the toxicity tests, overlying water in each chamber was drained to 1-cm depth on Day 0, and 10 clams (tagged for identification)[18] were placed evenly on the sediment surface, allowing them to remain semi-buried for easy survival checks. Seawater was then replenished to the original depth. Mortality was monitored every 12 h, and any dead clams were removed immediately. Surviving clams were collected on Day 10 for Cu analysis.

To monitor the bioaccumulation by the clams while maintaining relatively consistent clam density, a batchwise design was employed. Five batches (5 clams per replicate) were introduced on Days 0, 2, 4, 6, and 8, with each batch retrieved after 2 days. This approach, as opposed to a single introduction at the start and retrieval at different intervals, minimized bias from density-dependent bioturbation, which would occur if clam numbers declined progressively due to sampling. Before each batch was introduced, 10 clams were dissected to determine baseline Cu concentrations. Bioaccumulation over time was simulated from the combined results of all batches

(Section 2.6.2).

During sediment exposure, sediment samples were collected from each replicate at the start, and overlying water (10 mL, filtered and acidified) was sampled daily before and after manual renewal and dissolved Cu concentrations analyzed.

DGT samplers (DGT® Research Ltd.) were deployed in sediment on Days 0, 2, 4, 6, and 8. Each device consisted of a Chelex-100 binding gel, a polyacrylamide diffusive gel (0.8 mm thickness) and a 0.45 μm PES membrane (0.14 mm) in a piston-type plastic casing with a 3.14 cm^2 exposure window. Devices were inserted face-down into sediment (~0.5 cm depth) to accumulate Cu from porewater and exchangeable solid-phases, representing the labile Cu fraction potentially bioavailable to clams. After a 48-h deployment, the samplers were retrieved, rinsed with deionized water and stored at 4 °C until disassembly. Three additional DGT devices served as blanks, processed identically but not deployed, showed Cu concentrations <0.03 μg L^{-1} (assuming 48-h deployment), confirming no device contamination.

2.5 Characterization and chemical analysis

Detailed information on the analysis of sediments and DGTs is available in SI Note S1. Briefly, sediments were characterized for particle size distribution, dilute-acid (1 M HCl) extractable metal (AEM)[38] and total recoverable metal (TRM)[39] concentrations. DGT device was disassembled, and the Cu binding layer was digested in 1 mL of 1 M HNO_3 for 48 h. The eluent was then diluted and determined for Cu concentrations. DGT-labile Cu concentration was calculated according to the equations provided in the instruction manual (SI Note S2).

2.6 Data analysis

2.6.1 ^{65}Cu isotope tracing in aqueous exposure

In the aqueous exposure tests, the uptake and efflux of ^{65}Cu in the clams was traced by quantifying the change in newly accumulated ^{65}Cu concentrations in clam tissue ($[^{65}Cu]_{new}$, μg g^{-1}), calculated as:

$$[^{65}Cu]_{new} = \left([^{65}Cu]_{meas} - [^{63}Cu]_{meas}\right) \times 0.308 \quad (1)$$

where $[^{65}Cu]_{meas}$ and $[^{63}Cu]_{meas}$ (μg g^{-1}) are the tissue Cu concentration calculated using the measured concentrations of ^{65}Cu and ^{63}Cu isotopes, and 0.308 is the natural relative abundance of ^{65}Cu. For a detailed explanation of the derivation, please refer to our previous publications.[1,40]

2.6.2 Sediment Cu bioaccumulation

Cu bioaccumulation in sediments was quantified from the repeated 2-d batchwise bioassays throughout the exposure period. At each interval, the net accumulation rate (μg g^{-1} d^{-1}) was determined as the difference between clam tissue Cu at the end of deployment and baseline Cu concentrations, divided by the 2-d exposure duration.

To reconstruct whole-exposure accumulation dynamics, we applied a Monte Carlo resampling approach. For each time interval, 1000 random rate values were generated from normal distributions defined by the measured mean net accumulation rate and its standard deviation. Each simulated rate was multiplied by the 2-d interval to yield the corresponding net Cu uptake. To correct for elimination effects already embedded in the net rates, the values were divided by a factor of 0.947 (i.e., $1 - k_e$, with $k_e = 0.053$ d^{-1} from aqueous tests).

These corrected uptake values were then sequentially superimposed onto the baseline Cu concentrations, yielding a time series of tissue Cu burdens. This reconstructed series represents cumulative Cu uptake without efflux correction, and was subsequently fitted with the sediment TK model (excluding the elimination term).

2.7 TKTD model construction

The TKTD model describes bioaccumulation and toxicity through four key parameters: the uptake rate constant k_u, efflux rate constant k_e, mortality rate constant k_m, and internal toxicity threshold C_{IT}.

For the TK modelling of Cu uptake and elimination by the clams, the internal Cu concentration was controlled by the balance between uptake and elimination:[15]

$$\frac{dC_{int}(t)}{dt} = J_{in}(t) - k_e \times C_{int}(t) \quad (2)$$

where $C_{int}(t)$ is the tissue Cu concentration (μg g^{-1}) at time t, J_{in} is the Cu influx rate (μg g^{-1} d^{-1}), and k_e is the elimination rate constant (d^{-1}).

In the aqueous exposures, the influx ($J_{\mathrm{in}}^{\mathrm{aq}}$) was expressed as:

$$J_{\mathrm{in}}^{\mathrm{aq}}(t) = k_{\mathrm{u}} \times C_{\mathrm{w}}(t) \quad (3)$$

where k_{u} is the aqueous uptake rate constant (L g^{-1} d^{-1}) and C_{w} is the dissolved Cu concentration (μg L^{-1}).

For the sediment exposures, labile Cu concentrations measured by DGT (C_{DGT}) were used to represent the bioavailable fraction. At constant conditions, influx in sediment ($J_{\mathrm{in}}^{\mathrm{sed}}$) can be expressed analogously:

$$J_{\mathrm{in}}^{\mathrm{sed}}(t) = k_{\mathrm{DGT}} \times C_{\mathrm{DGT}}(t) \quad (4)$$

where k_{DGT} (L g^{-1} d^{-1}) is the uptake rate constant of DGT-labile Cu.

When C_{DGT} varies across a wide range, k_{DGT} is not a constant. To improve generality, the influx $J_{\mathrm{in}}^{\mathrm{sed}}$ was instead described by a power function:[1,41,42]

$$J_{\mathrm{in}}^{\mathrm{sed}}(t) = a \times C_{\mathrm{DGT}}^{b}(t) \quad (5)$$

where a and b are empirical constants. These parameter values were obtained by fitting the TK model without elimination to the reconstructed time series of tissue Cu burdens (Section 2.6.2).

For the TD modelling of toxic effects, a TD hazard model based on stochastic death assumption was used, which expects the hazard rate—instantaneous mortality risk—being proportional to excessive contaminant accumulation relative to an internal threshold:[15,43]

$$\frac{\mathrm{d}H(t)}{\mathrm{d}t} = \begin{cases} k_{\mathrm{m}} \times (C_{\mathrm{int}}(t) - C_{\mathrm{IT}}) + h_0 & \text{if } C_{\mathrm{int}}(t) > C_{\mathrm{IT}} \\ h_0 & \text{if } C_{\mathrm{int}}(t) \le C_{\mathrm{IT}} \end{cases} \quad (6)$$

$$S(t) = e^{-H(t)} \quad (7)$$

where H(t) is cumulative hazard (dimensionless), k_{m} is the mortality rate constant (mg μg^{-1} h^{-1}), C_{IT} is the internal threshold concentration (μg g^{-1}), h_0 is the background hazard rate (h^{-1}, set to 0), and $S(t)$ is the survival probability.

The physiological parameters k_{e}, k_{m}, and C_{IT}, which reflect species-specific traits, were obtained from aqueous exposure tests, while the influx parameters a and b were derived from sediment exposure tests. Model fitting was conducted in OpenModel (version 2.4.2, University of Nottingham) using least-squares estimation with the Marquardt algorithm, followed by optimization with Markov Chain Monte Carlo (MCMC) using the Metropolis-Hastings algorithm. Posterior parameter estimates are

reported as means ± standard deviations derived from MCMC posterior distribution (Table 1).

These parameters were then integrated into the sediment TKTD model to predict toxicity under sediment exposure. Predictions were generated by Monte Carlo simulations, drawing 1,000 random parameter sets from normal distributions defined by the estimated means and standard deviations. Simulations and statistical analyses were implemented in R (v4.3.1). Model performance was evaluated using Nash-Sutcliffe efficiency (NSE, $-\infty$ to 1.00, with 1.00 indicating perfect fit). Figures were produced using the ggplot2 package.

3. Results and Discussion

3.1 Aqueous Cu toxicokinetics and toxicodynamics

In the Aq-Low-Cu treatment, clams accumulated ^{65}Cu ($[^{65}Cu]_{new}$) to 1.8 μg g^{-1} after the 48-h isotope labeling. During the 16-d depuration, $[^{65}Cu]_{new}$ declined exponentially, with ~48% eliminated by the end of the period (Figure 1a). A one-compartment TK model adequately described the depuration kinetics (NSE = 0.86), with an efflux rate constant (k_e) of 0.053 d^{-1} (Figure 1a). This indicated that clams eliminated about 5.3% of their internal Cu burden per day.

In the Aq-High-Cu treatment, dissolved ^{65}Cu concentrations initially decreased from 406 to 269 μg L^{-1} within the first 24 h, likely due to adsorption onto container walls and clam shells (SI Figure S1). After the first water renewal (replaced with $CuCl_2$-spiked seawater), the decline slowed, and Cu concentrations stabilized between 340–430 μg L^{-1} for the remainder of the experiment.

Clams rapidly accumulated ^{65}Cu during the initial 24 h, reaching ~15 μg g^{-1} in tissue (Figure 1b, inset). Using the same elimination rate constant (k_e = 0.053 d^{-1}),[43] the uptake rate constant (k_u) was estimated at 0.046 L g^{-1} d^{-1} (Table 1).

High Cu exposure caused progressive mortality (Figure 1b). Deaths began on Day 2 and gradually declined. The survival curve was fitted using the TKTD model, which yielded an internal threshold concentration (C_{IT}) of 38.3 μg g^{-1} and a mortality rate constant (k_m) of 7.89 mg μg^{-1} d^{-1}. The threshold C_{IT} indicates that clams can

tolerate internal Cu burdens up to 38.3 μg g^{-1} without mortality risk, consistent with tissue analysis showing that most dead individuals exceed this value (SI Figure S2).

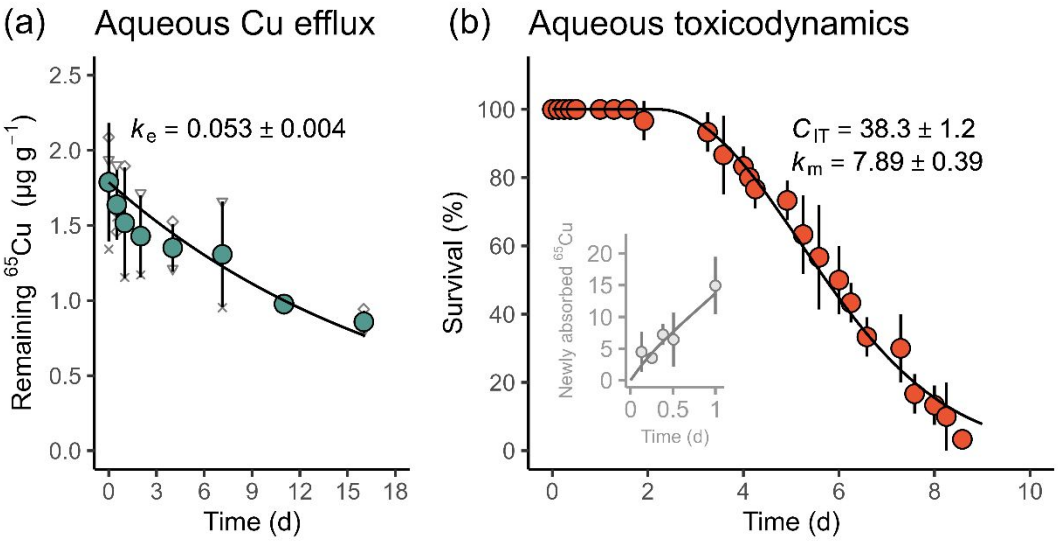

Figure 1. Aqueous toxicokinetics and toxicodynamics of Cu in clams. (a) Elimination kinetics in the Aq-Low-Cu treatment. The elimination rate constant (k_e) was obtained by fitting the model (black curve) to the time series of remaining ^{65}Cu in clams (large points: mean ± standard deviation, n = 3; small points: replicate means, each from two clams; (b) Survival kinetics in the Aq-High-Cu treatment. The internal threshold concentration (C_{IT}) and mortality rate constant (k_m) were derived from model-fit (black curve) to survival data (large points: mean ± standard deviation, n = 3). The inset shows accumulation of newly absorbed ^{65}Cu during the first day.

Table 1. TKTD model parameters. Values are reported as means ± standard deviations, where they were derived from posterior distributions estimated by MCMC fitting.

Exposure	Parameter	Unit	Equation or value
Aqueous	k_u	L g^{-1} d^{-1}	0.046 ± 0.004
	k_e	d^{-1}	0.053 ± 0.004
	C_{IT}	μg g^{-1}	38.3 ± 1.2
	k_m	mg μg^{-1} d^{-1}	7.90 ± 0.39
Sediment	J_{in}^{sed}	μg g^{-1} d^{-1}	$J_{in}^{sed} = a \times C_{DGT}^{b}$
	a	dimensionless	0.23 ± 0.00
	b	dimensionless	0.68 ± 0.00

3.2 Sediment Cu toxicokinetics and toxicodynamics

3.2.1 Sediment and water characteristics

The clean sediment used for Cu spiking was predominantly fine-grained, with 96% of particles <170 µm and 57% <64 µm (SI Table S1). TRM concentrations of Cu, Zn, Ni, Pb, and Cd were below sediment quality guideline values (SI Table S2), indicating that the sediment posed no significant risk to organism and was suitable as a control.

Cu-spiked sediments showed a total recoverable Cu (TR-Cu) concentration of 350 and 670 mg Cu kg^{-1} in the Sed-Low-Cu and Sed-High-Cu treatments, respectively (SI Table S3). Most of the added Cu was recovered by the dilute acid extractable fraction (AEM-Cu = 88% and 84% of the TR-Cu), suggesting that a high portion of the spiked Cu was potentially bioavailable to benthic organisms.[44,45]

Porewater DGT-labile Cu remained stable across treatments at 0.6 ± 0.2, 55 ± 11, and 223 ± 48 µg L^{-1} for the Sed-Control, Sed-Low-Cu, and Sed-High-Cu treatments, respectively (SI Figure S3). Overlying water Cu was elevated by release of Cu from the sediments (porewater flux) and remained an order of magnitude lower than porewater DGT-Cu values due to water renewal (SI Figure S3), averaging at 1.7 µg L^{-1} (Sed-Control), 8.0 µg L^{-1} (Sed-Low-Cu), and 38 µg L^{-1} (Sed-High-Cu).

3.2.2 Cu bioaccumulation in sediments

Batchwise (2-day) clam deployment produced net Cu accumulation rates consistent with sediment contamination levels (Figure 2a). In the Sed-Control with clean sediment, mean net rates were close to zero, ranging from –0.31 to 0.21 µg g^{-1} d^{-1}, with negative values indicating Cu loss.

In sediments the net accumulation rates increased with spiked-Cu concentration. The Sed-Low-Cu treatment showed mean rates of 2–4.4 µg g^{-1} d^{-1}, while the Sed-High-Cu treatment ranged from 5.8 to 11.1 µg g^{-1} d^{-1}. Rates were strongly correlated with DGT-labile Cu concentrations ($r = 0.97$, $p < 0.01$, SI Figure S4), confirming that DGT-labile Cu effectively reflected sediment Cu bioavailability.

Whole-exposure accumulation dynamics were constructed by superimposing the

corrected 2-day uptake increments using the Monte Carlo method. The resulting time series of reconstructed tissue Cu burdens showed consistent trends with sediment Cu bioavailability. In the Sed-Control treatment, tissue Cu remained close to baseline concentrations (Figure 2b), while in the Sed-Low-Cu and Sed-High-Cu treatments, burdens increased steadily to 44 and 99 μg g^{-1}, respectively (Figure 2b).

The reconstructed tissue Cu burdens were fitted with the sediment TK model without an elimination term (Equation 5), yielding uptake parameters of $a = 0.23$ and $b = 0.68$ (Figure 2b, dashed curves). When the efflux term was reintroduced, the model predicted tissue Cu concentrations (Figure 2b, solid curves) at the end of the sediment exposure phase as 5.3, 32, and 76 μg g^{-1} for the Sed-Control, Sed-Low-Cu, and Sed-High-Cu treatments, respectively (Figure 2c). These predictions aligned well with the measured values from the survived clams, with comparable levels in the Sed-Low-Cu (32 vs. 29 μg g^{-1}, $p = 0.058$) and Sed-High-Cu treatments (77 vs. 77 μg g^{-1}, $p = 0.996$), while a slight underestimation (within 2-fold) in the Sed-Control treatment (5.3 vs. 7.9 μg g^{-1}) (Figure 2c). Overall, these results confirm that the stepwise reconstruction and TK modeling approach effectively captured Cu bioaccumulation in sediments.

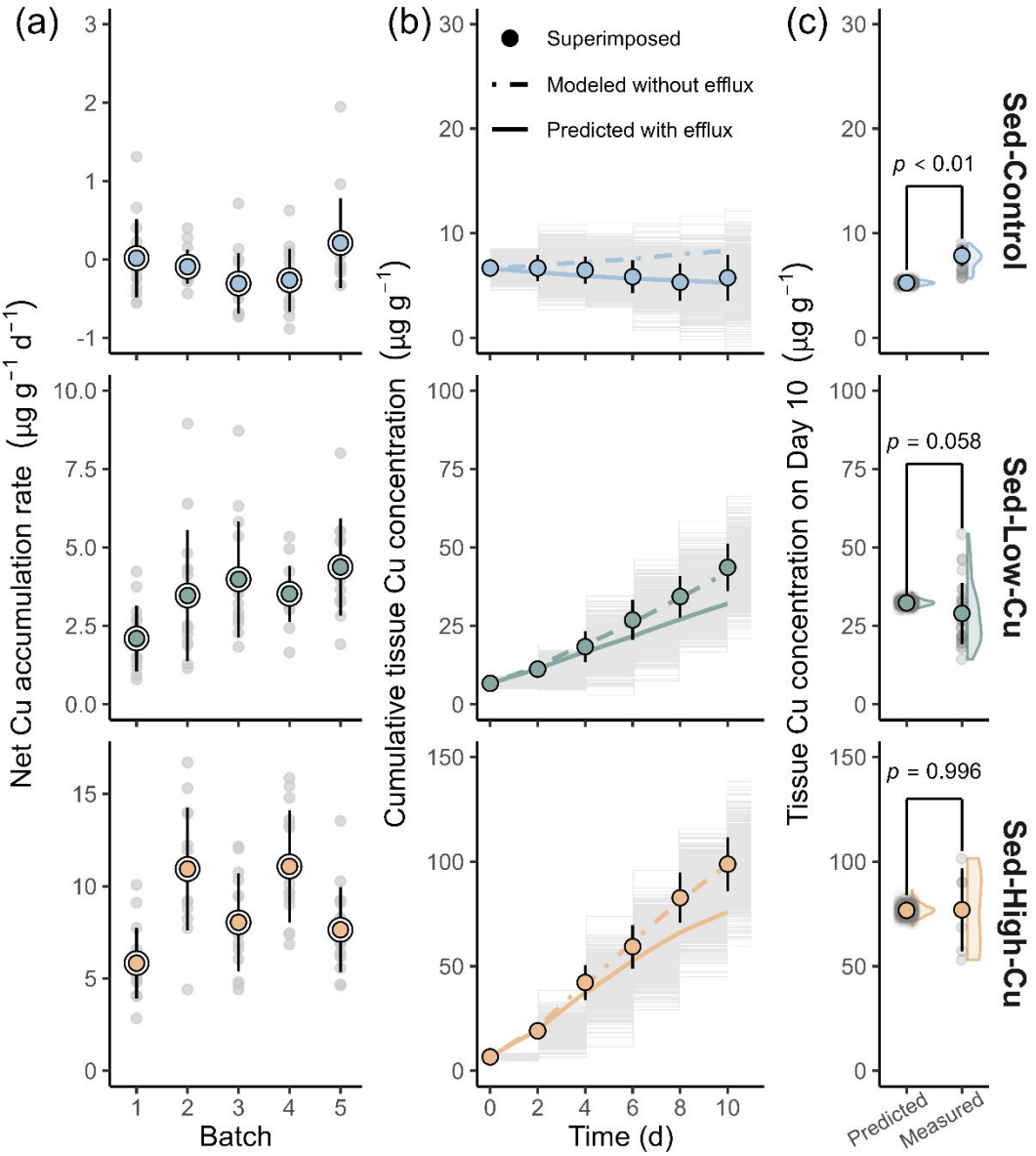

Figure 2. Sediment Cu bioaccumulation kinetics and model validation in clams. (a) Net Cu accumulation rates across treatments. Solid colored points show mean ± standard deviation (n = 15), with grey points representing individual accumulation rates. (b) Superimposed and model-predicted tissue Cu concentrations during exposure. The stepwise grey segments show simulated concentrations at 2-day intervals (Monte Carlo simulation, n = 1000) sequentially superimposed onto the baseline Cu concentrations. Solid points with error bars represent mean ± standard of the simulated concentrations. The dashed curve represents the fit to these simulated concentrations using TK model excluding the efflux term, while the solid curve represents predicted tissue concentration when efflux was reintroduced (refer to Section 2.6.2 for method details). (c) Comparison between predicted and measured tissue concentration at the end of exposure. Half-violin plots show the distribution of predicted and measured tissue concentrations (grey dots: individual values). Welch's t-test indicated no significant difference between the two groups in the Sed-Low-Cu and Sed-High-Cu treatments.

3.2.3 Cu toxicity prediction

Clam survival remained unaffected in the Sed-Control and Sed-Low-Cu treatments. In contrast, in the Sed-High-Cu treatment, mortality commenced on Day 3 and increased steadily to 77% (23% survival) by the end of sediment exposure (Figure 3a).

The sediment TKTD model reproduced the survival patterns with moderate accuracy (NSE = 0.74; Figure 3a). The model predicted progressive mortality in the Sed-High-Cu treatment, with mortality onset on Day 4 (Figure 3a). However, survival was consistently overestimated, underpredicting toxicity by ~10% (Figure 3a, inset).

A sensitivity analysis was conducted to explore possible sources of discrepancy (Figure 3b-d). Decreasing k_e or increasing k_m improved model prediction at later stages (after Day 7), but these adjustments did not shift the timing of toxicity onset. In contrast, lowering the internal threshold concentration (C_{IT}) substantially improved the overall prediction. Reducing C_{IT} from 40 to 30 μg g^{-1} increased NSE from 0.69 to 0.97, with the optimum C_{IT} estimated at 28.1 μg g^{-1}.

The lower optimum C_{IT} under sediment exposure (28.1 μg g^{-1}) compared to aqueous exposure (38.3 μg g^{-1}) suggests that *R. philippinarum* became more sensitive to internalized Cu under sediment exposure. A similar reduction in threshold sensitivity has been reported for benthic clam *Potamocorbula laevis* exposed to Cu-bearing suspended particulate matter, where C_{IT} decreased by ~54% (from 141 to 76.8 μg g^{-1}).[46] This enhanced sensitivity is likely linked to additional stressors imposed by fine sediments, including feeding-structure clogging, respiratory-organ damage, or osmotic dysfunction.[47–49]

Overall, while the TKTD model using aqueous-derived parameters alone may underestimate sediment toxicity, the discrepancy (~10%) was within the uncertainty typically observed for sublethal endpoints in sediment toxicity studies (e.g., 15% uncertainty commonly found in reproduction measurement).[25,50] This gap can be addressed by applying a conservative modifying factor, for example by adjusting the aqueous-derived C_{IT} downward by ~27% (i.e., multiplied by 0.73) to better reflect sensitivity under sediment exposure conditions.

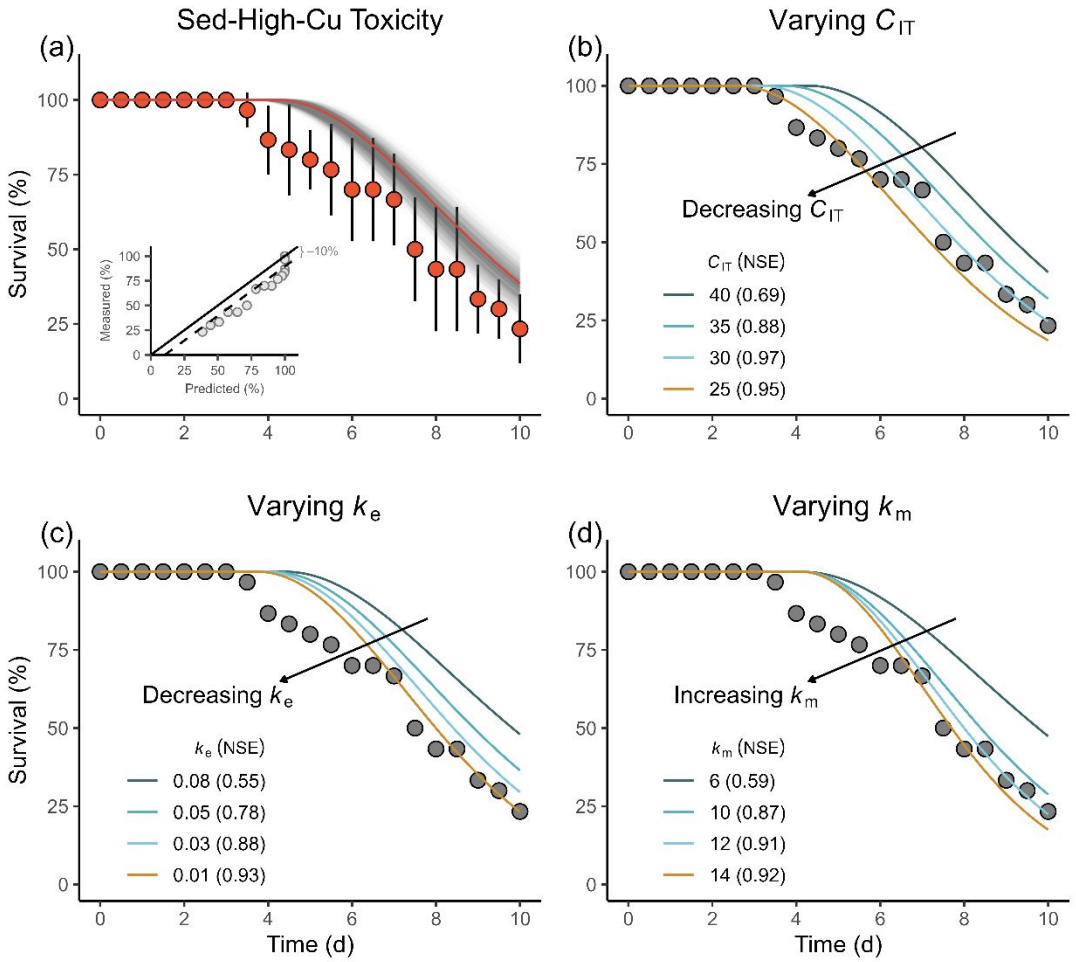

Figure 3. Observed and predicted clam survival in the Sed-High-Cu treatment. (a) The model using aqueous-derived parameters (k_e, C_{IT}, k_m) slightly underestimated toxicity to clam survival. Red points show observed survival (mean ± standard deviation, n = 3). Grey curves are Monte Carlo predictions, with the red curve as the mean. The inset compares predicted and observed mean survival, showing an average underestimation of 10%. (b-d) Sensitivity analysis of individual parameters. Decreasing k_e improves overall prediction (b), while decreasing C_{IT} or increasing k_m improves late-stage prediction (c, d). Model performance (NSE) is shown in the legend (values in brackets).

3.3 Derivation of acute-to-chronic ratio (ACR)

3.3.1 ACR for Cu induced mortality of R. philippinarum

The TKTD model was applied to derive a chronic safety threshold for sediment-associated Cu, expressed as the no-effect concentration based on DGT-labile Cu (NEC_{Cu}). This threshold represents the maximum Cu exposure concentration that does not induce mortality during long-term exposure. The NEC_{Cu} was derived under two

steady state assumptions: (i) tissue Cu concentration reaches equilibrium ($\frac{dC_{int}(t)}{dt} = 0$), and (ii) internal Cu burden remains below the critical threshold ($C_{int} \leq C_{IT}$). Solving the TKTD equation with parameter values (Table 1) yielded an NEC_{Cu} of 23.6 µg L^{-1} (Figure 4a). When the adjusted-C_{IT} value (28.1 µg g^{-1}, derived from sensitivity analysis) was applied, the NEC_{Cu} decreased to 15.0 µg L^{-1}. Below this concentration, long-term Cu exposure is not expected to induce clam mortality.

Acute toxicity thresholds were also determined. While the LC_{50} can be visually estimated from the observed acute toxicity profile (median mortality onset between Days 7 to 8, Figure 3a), the TKTD model provided a more consistent, time-dependent estimate that avoids dependence on a single test duration (Figure 4b). Model simulations (R code provided in Note S2, SI) predict that LC_{50} values decrease rapidly with exposure time before stabilizing near 27 µg L^{-1} after 100 days. For the 7-d exposure, the predicted LC_{50}-7d was 401 µg L^{-1}.

The ACR was then defined as the ratio of the acute LC_{50}-7d to the chronic NEC_{Cu}. This yielded an ACR of 17 using the unadjusted NEC and 27 when the adjusted NEC was applied (Figure 4b). These ACR values are specific to *R. philippinarum* exposed to sediment-associated Cu, with mortality as the common endpoint for both acute and chronic thresholds.

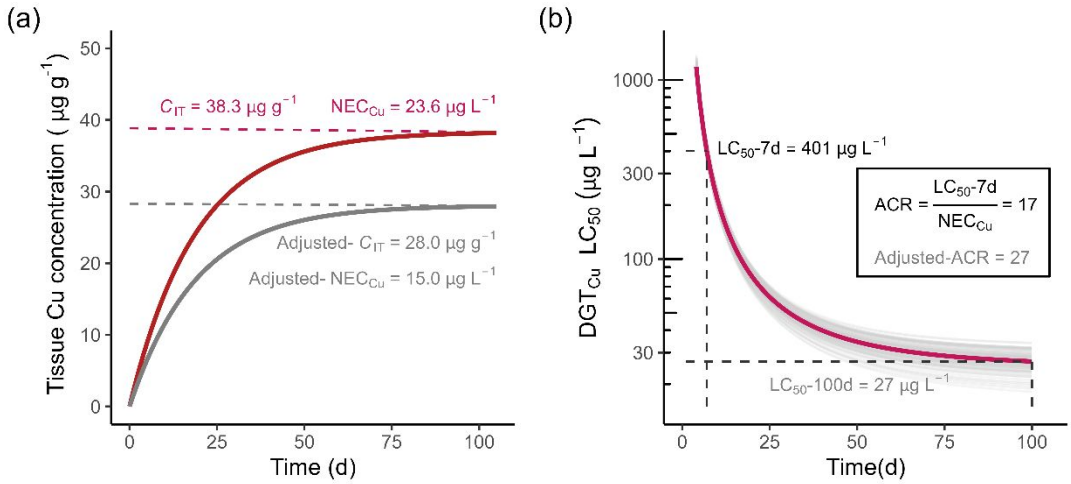

Figure 4. Derivation of acute-to-chronic ratio (ACR) from the sediment TKTD model. (a) Long-term no-effect concentration (NEC_{Cu}) The red curve shows Cu accumulation in clam tissue under exposure to 23.6 µg L^{-1} DGT-labile Cu, reaching the C_{IT} threshold at steady state. The grey curve shows predictions using an adjusted-

C_{IT} (28.0 µg g^{-1}, derived from sensitivity analysis). (b) Predicted median lethal concentration (LC_{50}) as a function of time. The thin curves (n = 100) and the bold red curve (average) shows predicted time-varying LC_{50}. The ACR was calculated as the ratio of 7-d LC_{50} to NEC_{Cu}.

3.3.2 ACRs for other contaminants using literature-derived TKTD parameters

Beyond Cu-induced mortality in *R. philippinarum*, we applied the TKTD framework to derive ACRs for other contaminants and species using literature-reported model parameters (SI Note S3). The selected studies were primarily based on TKTD models that implement toxicodynamics under stochastic mortality assumptions (similar to our present framework). While numerous other TKTD studies exist, many employ different model structures (e.g., alternative toxicodynamic formulations or TK specifications), which complicate direct ACR derivation and comparison. Our aim here was therefore not to provide an exhaustive review of TKTD applications, but rather to demonstrate the feasibility and advantages of mechanistically deriving ACRs across different contaminants and species. As most TKTD work has been developed under aqueous exposure conditions, they were directly adopted, while acknowledging that sediment-specific applications remain limited. The derivation of ACRs followed the same principles demonstrated for sediment-associated Cu, with LC_{50} values obtained from time-dependent survival predictions and NEC values determined from internal threshold constraints (SI Table S4).

The derived ACRs varied widely across contaminants and species (Figure 5). For Cu, studies with the benthic clam *Potamocorbula laevis* yielded ACRs in the range of 1.8–6.6,[43,46] generally comparable to our sediment-based estimates for *R. philippinarum* (17). In contrast, Cd showed consistently higher values (11–87) across both clam and zooplankton studies,[1,51,52] indicating a broader margin between acute and chronic effects relative to Cu. Nanoplastic particles exhibited high variability, with ACRs ranging from 1.8 to 69, reflecting differences in particle size, organism tested, and modeled endpoint (mortality or growth inhibition).[53–55] Overall, these comparisons suggest a degree of contaminant-specificity in ACR values, with Cu generally producing lower factors, Cd consistently higher, and both Cd and

nanoplastics spanning a broad range.

A notable advantage of the mechanistic framework is its ability to investigate how environmental conditions influence ACRs. For example, in studies of *P. laevis* exposed to Cu and Cd under varying salinity,[1,43] we found that ACR values decreased with increasing salinity: from 2.7 to 1.8 for Cu, and from 39 to 11 for Cd as salinity increased from 5 to 30. The stronger sensitivity of Cd to salinity aligns with established knowledge that cadmium speciation, and hence bioavailability, is more strongly affected by chloride complexation than copper.[17] Similarly, in the case of nanoplastics, the derived ACRs tended to decline with increasing particle size, consistent with the idea that smaller particles exhibit higher uptake efficiency and more pronounced chronic effects.[56]

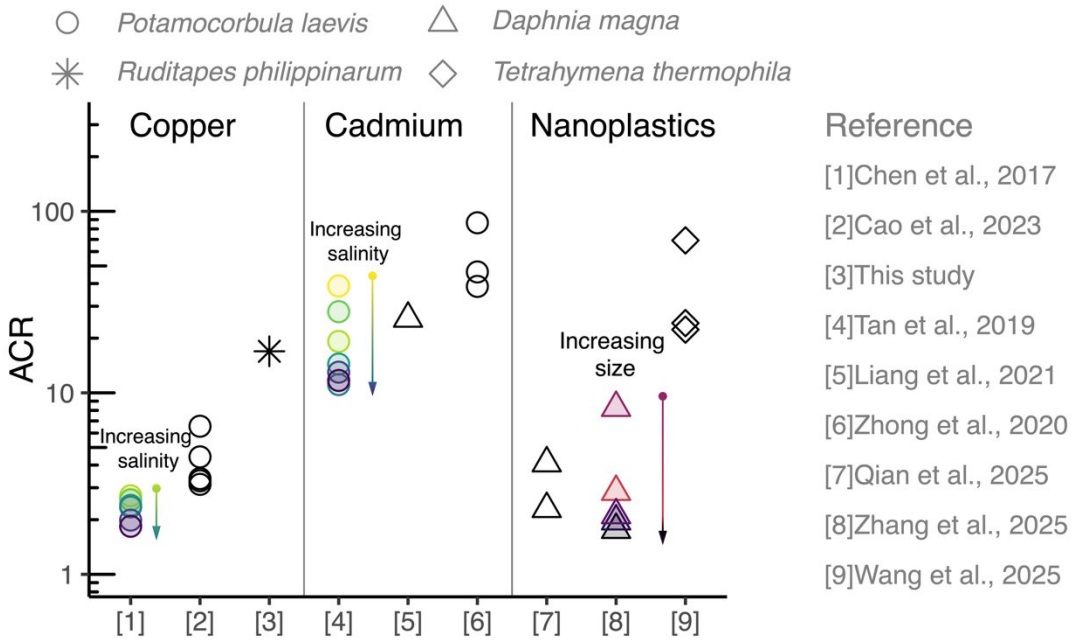

Figure 5. ACR values derived for other contaminants, species, and environmental conditions. Different point shapes represent the four species, while color gradients indicate variations in salinity and nanoplastic size. For a complete list of references, please refer to the Supporting Information Table S4.

3.4 Merits, limitations, and implications of the mechanistic approach

Ecological risk assessment typically follows a tiered framework, where extrapolation factors play a key role in bridging the gap between laboratory-derived effects data and prediction of long-term ecosystem-level protection.[7,9,38,57] The

effective application of these factors in regulations requires careful consideration: factors that are too small risk allowing hazardous chemicals to sneak through assessment without adequate scrutiny, while factors that are too large may slow the assessment process by pushing unnecessary cases into higher-tier testing or management actions.[4,7] The ACR is one such extrapolation factor, and its reliability ultimately shapes the efficiency and protectiveness of the assessment process.[7]

Compared with conventional approaches, the modeling-based ACR derivation offers two distinct advantages. First, it grounds the extrapolation in mechanistic processes of uptake, elimination, and effect, which reduces reliance on cross-study comparisons of mismatched acute and chronic datasets. Second, by explicitly capturing time-dependent toxicity, it provides a transparent and reproducible way to relate acute experiments of different durations to chronic thresholds. This transparency is particularly valuable because it allows the derived ACR to be traced back to underlying processes and thus allowing comparison under variable environmental conditions. For example, toxicokinetic modeling has shown environmental factors such as salinity,[1,43,52] temperature,[58,59] sediment resuspension[60] influence contaminant bioaccumulation. While their effects on toxicodynamics and ACRs are less well understood, our extended analysis (Section 3.3) illustrates how mechanistically derived ACRs can capture such variability. Specifically, systematic differences were observed across contaminants (e.g., Cu vs. Cd), species (e.g., clams vs. zooplankton), and even under changing salinity conditions, highlighting how chemical properties and environmental drivers jointly shape acute-to-chronic relationships. Such insights are not achievable through traditional empirical factors, underscoring the added value of mechanistic derivation.

In principle, the framework could deliver species-specific ACRs for a wide range of contaminants, offering a refined alternative to current empirical factors. In practicality, however, the bottleneck lies in the effort required to parameterize models across many species. A pragmatic compromise is to focus on key test species that are either ecologically relevant or have a long history of regulatory use. More efficiently, mechanistic ACRs could be derived for several of the more sensitive species

identified from species sensitivity distributions (SSDs), effectively serving as a "patch" to strengthen current regulatory approaches. Even this limited application could enhance the scientific robustness of sediment or water quality criteria, while keeping data and modeling requirements at a manageable level.

The present study focused on mortality because of its experimental feasibility and the relative simplicity of modeling survival data. Consequently, the derived ACRs primarily address uncertainty associated with this endpoint. An implicit premise of this approach is that acute and chronic risks are governed by the same toxicity mechanism, with differences arising mainly from exposure duration. In reality, however, chronic risks may shift toward sublethal effects, such as impaired growth or reproduction, which are not captured when mortality is used as the sole endpoint. Incorporating these processes would improve ecological relevance and provide a more comprehensive basis for extrapolation. This is feasible using more complex toxicodynamic frameworks, such as DEBtox, which capture energy allocation and life-history traits.[61,62] Yet, these models require specifically designed experiments and detailed physiological data, which may constrain their regulatory application.[63,64] Our work therefore represents a practical approach for mechanistic ACR derivation, with future progress to expand toward sublethal endpoints as modeling approaches and datasets mature.

In conclusion, this study developed a mechanistic toxicokinetic-toxicodynamic (TKTD) framework to derive the acute-to-chronic ratio (ACR) for the benthic clam *Ruditapes philippinarum* exposed to sediment-associated Cu. By transferring physiological parameters (k_e, C_{IT}, k_m) calibrated from aqueous tests and using DGT-labile Cu as a proxy for the bioavailable fraction in sediments, we established a tractable modeling approach that adequately reproduced observed toxicity under sediment exposure. The framework yielded an ACR of 17 for mortality, linking acute and chronic effects in a process-based manner. These results provide a strong proof of concept that TKTD modeling can strengthen ecological risk assessment by replacing empirical extrapolation with a transparent, mechanistically grounded basis for safety factors, thereby improving both robustness and regulatory relevance.

ACKNOWLEDGEMENTS

We thank Hongkai Wang, Haiyan Xiong, Jieru Lin and Jing Qian for their assistance with the laboratory experiment, and Dr. Fang Wu for her assistance with the ICP-MS analysis. This study was supported by the National Natural Science Foundation of China (Grant No.42477281, 42377267).

Reference

(1) Tan, Q.-G.; Lu, S.; Chen, R.; Peng, J. Making acute tests more ecologically relevant: cadmium bioaccumulation and toxicity in an estuarine clam under various salinities modeled in a toxicokinetic–toxicodynamic framework. *Environ. Sci. Technol.* **2019**, *53* (5), 2873–2880.

(2) Calow, P.; Forbes, V. E. Does ecotoxicology inform ecological risk assessment? *Environ. Sci. Technol.* **2003**, *37* (7), 146A-151A.

(3) Länge, R.; Hutchinson, T. H.; Scholz, N.; SolbÉ, J. Analysis of the ECETOC aquatic toxicity (EAT) database II — comparison of acute to chronic ratios for various aquatic organisms and chemical substances. *Chemosphere* **1998**, *36* (1), 115–127.

(4) Chapman, P. M.; Fairbrother, A.; Brown, D. A critical evaluation of safety (uncertainty) factors for ecological risk assessment. *Environ. Toxicol. Chem.* **1998**, *17* (1), 99–108.

(5) Zolezzi, M.; Cattaneo, C.; Tarazona, J. V. Probabilistic ecological risk assessment of 1, 2, 4-trichlorobenzene at a former industrial contaminated site. *Environ. Sci. Technol.* **2005**, *39* (9), 2920–2926.

(6) Warne, M. S. J.; Batley, G. E.; van Dam, R.; Chapman, J.; Fox, D.; Hickey, C.; Stauber, J. *Revised method for deriving Australian and New Zealand water quality guideline values for toxicants*; Queensland Department of Science, Information Technology, Innovation and the Arts: Brisbane, Australia, **2015**.

(7) Forbes, V. E.; Calow, P. Extrapolation in ecological risk assessment: balancing pragmatism and precaution in chemical controls legislation: extrapolation is a practical necessity in ecological risk assessment, but there is much room for improvement in the extrapolation process. *BioScience* **2002**, *52* (3), 249–257.

(8) ECETOC. *Aquatic hazard assessment II. ECETOC technical report number 91*; European Centre for Ecotoxicology and Toxicology of Chemicals: Brussels, **2003**.

(9) Duke, L. D.; Taggart, M. Uncertainty factors in screening ecological risk assessments. *Environ. Toxicol. Chem.* **2000**, *19* (6), 1668–1680.

(10) ECETOC. *Aquatic toxicity data evaluation. ECETOC technical report number 56*; Aquatic toxicity data evaluation; European Centre for Ecotoxicology and

Toxicology of Chemicals: Brussels, **1993**.

(11) USEPA. *Aquatic Life Ambient Water Quality Criteria Cadmium−2016*; Washington, DC, **2016**.

(12) Calabrese, E. J.; Baldwin, L. A. *Performing Ecological Risk Assessments*; Lewis Publishers: Chelsea, MI, **1993**.

(13) Roex, E. W. M.; Van Gestel, C. A. M.; Van Wezel, A. P.; Van Straalen, N. M. Ratios between acute aquatic toxicity and effects on population growth rates in relation to toxicant mode of action. *Environ. Toxicol. Chem.* **2000**, *19* (3), 685–693.

(14) Jager, T.; Albert, C.; Preuss, T. G.; Ashauer, R. General unified threshold model of survival-a toxicokinetic-toxicodynamic framework for ecotoxicology. *Environ. Sci. Technol.* **2011**, *45* (7), 2529–2540.

(15) Tan, Q.-G.; Wang, W.-X. Two-compartment toxicokinetic–toxicodynamic model to predict metal toxicity in *Daphnia magna*. *Environ. Sci. Technol.* **2012**, *46* (17), 9709–9715.

(16) Wang, W.-X.; Tan, Q.-G. Applications of dynamic models in predicting the bioaccumulation, transport and toxicity of trace metals in aquatic organisms. *Environ. Pollut.* **2019**, *252*, 1561–1573.

(17) Luoma, S.; Rainbow, P. S. *Metal contamination in aquatic environments: science and lateral management*; Cambridge University Press: Cambridge, UK, **2008**.

(18) Su, Q.; Xiao, W.; Simpson, S. L.; Tan, Q.-G.; Chen, R.; Xie, M. Enhancing sediment bioaccumulation predictions: isotopically modified bioassay and biodynamic modeling for nickel assessment. *Environ. Sci. Technol.* **2023**, *57* (48), 19352–19362.

(19) Zhang, C.; Yu, Z.; Zeng, G.; Jiang, M.; Yang, Z.; Cui, F.; Zhu, M.; Shen, L.; Hu, L. Effects of sediment geochemical properties on heavy metal bioavailability. *Environ. Int.* **2014**, *73*, 270–281.

(20) Strom, D.; Simpson, S. L.; Batley, G. E.; Jolley, D. F. The influence of sediment particle size and organic carbon on toxicity of copper to benthic invertebrates in oxic/suboxic surface sediments. *Environ. Toxicol. Chem.* **2011**, *30* (7), 1599–1610.

(21) Zhang, H.; Davison, W.; Miller, S.; Tych, W. In situ high resolution measurements of fluxes of Ni, Cu, Fe, and Mn and concentrations of Zn and Cd in porewaters by DGT. *Geochim. Cosmochim. Acta* **1995**, *59* (20), 4181–4192.

(22) Zhang, H.; Davison, W.; Mortimer, R. J. G.; Krom, M. D.; Peter J. Hayes; Davies, I. M. Localised remobilization of metals in a marine sediment. *Sci. Total Environ.* **2002**, *296* (1), 175–187.

(23) Xie, M.; Simpson, S. L.; Huang, J.; Teasdale, P. R.; Wang, W.-X. In situ DGT sensing of bioavailable metal fluxes to improve toxicity predictions for sediments. *Environ. Sci. Technol.* **2021**, *55* (11), 7355–7364.

(24) Simpson, S. L.; Yverneau, H.; Cremazy, A.; Jarolimek, C. V.; Price, H. L.; Jolley, D. F. DGT-induced copper flux predicts bioaccumulation and toxicity to bivalves in sediments with varying properties. *Environ. Sci. Technol.* **2012**, *46* (16), 9038–9046.

(25) Amato, E. D.; Simpson, S. L.; Jarolimek, C. V.; Jolley, D. F. Diffusive gradients in thin films technique provide robust prediction of metal bioavailability and toxicity in estuarine sediments. *Environ. Sci. Technol.* **2014**, *48* (8), 4485–4494.

(26) Choi, J. Y.; Yu, J.; Yang, D. B.; Ra, K.; Kim, K. T.; Hong, G. H.; Shin, K. H. Acetylthiocholine (ATC) – cleaving cholinesterase (ChE) activity as a potential biomarker of pesticide exposure in the Manila clam, *Ruditapes philippinarum*, of Korea. *Mar. Environ. Res.* **2011**, *71* (3), 162–168.

(27) Ji, C.; Cao, L.; Li, F. Toxicological evaluation of two pedigrees of clam *Ruditapes philippinarum* as bioindicators of heavy metal contaminants using metabolomics. *Environ. Toxicol. Pharmacol.* **2015**, *39* (2), 545–554.

(28) Wang, Z.; Yan, C.; Vulpe, C. D.; Yan, Y.; Chi, Q. Incorporation of in situ exposure and biomarkers response in clams *Ruditapes philippinarum* for assessment of metal pollution in coastal areas from the Maluan Bay of China. *Mar. Pollut. Bull.* **2012**, *64* (1), 90–98.

(29) Chong, K.; Wang, W. Bioavailability of sediment-bound Cd, Cr and Zn to the green mussel *Perna viridis* and the Manila clam *Ruditapes philippinarum*. *J. Exp. Mar. Biol. Ecol.* **2000**, *255* (1), 75–92.

(30) Woody, C. A.; O'Neal, S. *Effects of copper on fish and aquatic resources*; Fisheries Research and Consulting Anchorage: Alaska, AK, USA, **2012**.

(31) Birch, G. F.; Lee, J.-H.; Tanner, E.; Fortune, J.; Munksgaard, N.; Whitehead, J.; Coughanowr, C.; Agius, J.; Chrispijn, J.; Taylor, U.; Wells, F.; Bellas, J.; Besada, V.; Viñas, L.; Soares-Gomes, A.; Cordeiro, R. C.; Machado, W.; Santelli, R. E.; Vaughan, M.; Cameron, M.; Brooks, P.; Crowe, T.; Ponti, M.; Airoldi, L.; Guerra, R.; Puente, A.; Gómez, A. G.; Zhou, G. J.; Leung, K. M. Y.; Steinberg, P. Sediment metal enrichment and ecological risk assessment of ten ports and estuaries in the World Harbours Project. *Mar. Pollut. Bull.* **2020**, *155*, 111129.

(32) Gao, X.; Liu, Z.; Li, J.; Wang, X.; Cui, L.; Ai, S.; Zhao, S.; Xu, Q. Ecological and health risk assessment of perfluorooctane sulfonate in surface and drinking water resources in China. *Sci. Total Environ.* **2020**, *738*, 139914.

(33) Johnson, A. C.; Jin, X.; Nakada, N.; Sumpter, J. P. Learning from the past and considering the future of chemicals in the environment. *Science* **2020**, *367* (6476), 384–387.

(34) Lu, Y.; Wang, P.; Wang, C.; Zhang, M.; Cao, X.; Chen, C.; Wang, C.; Xiu, C.; Du, D.; Cui, H.; Li, X.; Qin, W.; Zhang, Y.; Wang, Y.; Zhang, A.; Yu, M.; Mao, R.; Song, S.; Johnson, A. C.; Shao, X.; Zhou, X.; Wang, T.; Liang, R.; Su, C.;

Zheng, X.; Zhang, S.; Lu, X.; Chen, Y.; Zhang, Y.; Li, Q.; Ono, K.; Stenseth, N. C.; Visbeck, M.; Ittekkot, V. Multiple pollutants stress the coastal ecosystem with climate and anthropogenic drivers. *J. Hazard. Mater.* **2022**, *424*, 127570.

(35) Yang, L.; Li, S.; Zhang, R. Copper threatens marine ecosystems. *Science* **2025**, *389* (6763), 884–884.

(36) Pan, K.; Wang, W.-X. Trace metal contamination in estuarine and coastal environments in China. *Sci. Total Environ.* **2012**, *421–422*, 3–16.

(37) Hutchins, C. M.; Teasdale, P. R.; Lee, S. Y.; Simpson, S. L. Cu and Zn concentration gradients created by dilution of pH neutral metal-spiked marine sediment: a comparison of sediment geochemistry with direct methods of metal addition. *Environ. Sci. Technol.* **2008**, *42* (8), 2912–2918.

(38) Simpson, S.; Batley, G. *Sediment quality assessment: a practical guide*; CSIRO Publishing: Melbourne, Victoria, Australia, **2016**.

(39) USEPA. *Method 3051A. Microwave assisted acid digestion of sediments, sludges, soils, and oils*; Washington, DC, **2007**.

(40) Wu, Q.; Zheng, T.; Simpson, S. L.; Tan, Q.-G.; Chen, R.; Xie, M. Application of a multi-metal stable-isotope-enriched bioassay to assess changes to metal bioavailability in suspended sediments. *Environ. Sci. Technol.* **2021**, *55* (19), 13005–13013.

(41) Wang, W.; Fisher, N.; Luoma, S. Kinetic determinations of trace element bioaccumulation in the mussel *Mytilus edulis*. *Mar. Ecol. Prog. Ser.* **1996**, *140*, 91–113.

(42) Shi, D.; Wang, W.-X. Understanding the differences in Cd and Zn bioaccumulation and subcellular storage among different populations of marine clams. *Environ. Sci. Technol.* **2004**, *38* (2), 449–456.

(43) Chen, W.-Q.; Wang, W.-X.; Tan, Q.-G. Revealing the complex effects of salinity on copper toxicity in an estuarine clam *Potamocorbula laevis* with a toxicokinetic-toxicodynamic model. *Environ. Pollut.* **2017**, *222*, 323–330.

(44) Simpson, S. L.; Spadaro, D. A. Bioavailability and chronic toxicity of metal sulfide minerals to benthic marine invertebrates: implications for deep sea exploration, mining and tailings disposal. *Environ. Sci. Technol.* **2016**, *50* (7), 4061–4070.

(45) Simpson, S. L.; Spadaro, D. A.; O'Brien, D. Incorporating bioavailability into management limits for copper in sediments contaminated by antifouling paint used in aquaculture. *Chemosphere* **2013**, *93* (10), 2499–2506.

(46) Cao, X.; Yu, Z.-X.; Xie, M.; Pan, K.; Tan, Q.-G. Higher risks of copper toxicity in turbid waters: quantifying the bioavailability of particle-bound metals to set site-specific water quality criteria. *Environ. Sci. Technol.* **2023**, *57* (2), 1060–1070.

(47) Bilotta, G. S.; Brazier, R. E. Understanding the influence of suspended solids on

water quality and aquatic biota. *Water Res.* **2008**, *42* (12), 2849–2861.

(48) Cheung, S. G.; Shin, P. K. S. Size effects of suspended particles on gill damage in green-lipped mussel *Perna viridis*. *Mar. Pollut. Bull.* **2005**, *51* (8–12), 801–810.

(49) Crémazy, A.; Wood, C. M.; Smith, D. S.; Val, A. L. The effects of natural suspended solids on copper toxicity to the cardinal tetra in Amazonian River waters. *Environ. Toxicol. Chem.* **2019**, *38* (12), 2708–2718.

(50) Zhang, Y.; Xie, M.; Spadaro, D. M.; Simpson, S. L. Improving toxicity prediction of metal-contaminated sediments by incorporating sediment properties. *Environ. Pollut.* **2023**, *338*, 122708.

(51) Liang, W.-Q.; Xie, M.; Tan, Q.-G. Making the Biotic Ligand Model kinetic, easier to develop, and more flexible for deriving water quality criteria. *Water Res.* **2021**, *188*, 116548.

(52) Zhong, G.; Lu, S.; Chen, R.; Chen, N.; Tan, Q.-G. Predicting risks of cadmium toxicity in salinity-fluctuating estuarine waters using the toxicokinetic–toxicodynamic model. *Environ. Sci. Technol.* **2020**, *54* (21), 13899–13907.

(53) Qian, H.; Wang, Y.; Wang, Y.; Hu, H.; Tan, Q.-G.; Yan, N.; Xie, M. Numeric uptake drives nanoplastic toxicity: size-effects uncovered by toxicokinetic-toxicodynamic (TKTD) modeling. *J. Hazard. Mater.* **2025**, *486*, 137105.

(54) Zhang, K.-D.; Wang, Z.; Zhang, H.-J.; Fang, H.-T.; Tan, Q.-G.; Miao, A.-J. Toxicokinetic-toxicodynamic modeling reveals the ecological risks of differently-sized polystyrene nanoplastics. *Environ. Pollut.* **2025**, *383*, 126792.

(55) Wang, M.; Fang, H.-T.; Tan, Q.-G.; Ji, R.; Miao, A.-J. Size-dependent toxicity of polystyrene nanoplastics to *Tetrahymena thermophila*: a toxicokinetic–toxicodynamic assessment. *Environ. Sci. Technol.* **2025**, *59* (21), 10194–10203.

(56) Liu, W.; Liao, H.; Wei, M.; Junaid, M.; Chen, G.; Wang, J. Biological uptake, distribution and toxicity of micro(nano)plastics in the aquatic biota: a special emphasis on size-dependent impacts. *TrAC Trends Anal. Chem.* **2024**, *170*, 117477.

(57) Solomon, K. R.; Brock, T. C. M.; Zwart, D. D.; Dyer, S. D.; Posthuma, L.; Richards, S. M.; Sanderson, H.; Sibley, P. K.; Van Den Brink, P. J. *Extrapolation practice for ecotoxicological effect characterization of chemicals*; CRC Press, **2008**.

(58) Tsui, M. T. K.; Wang, W.-X. Temperature influences on the accumulation and elimination of mercury in a freshwater cladoceran, *Daphnia magna*. *Aquat. Toxicol.* **2004**, *70* (3), 245–256.

(59) Ma, X.; Xiao, W.; Zhang, Q.; Yu, Z.; Jia, X.; Chen, R.; Xie, M.; Tan, Q.-G. Fast in, faster out: rapid thallium elimination drives low bioaccumulation in coastal gastropods. *Environ. Sci. Technol.* **2025**, *59* (30), 15720–15729.

(60) Xu, D.; Xiong, H.; Wu, Q.; Xiao, W.; Simpson, S. L.; Tan, Q.-G.; Chen, R.; Xie,

M. Sediment ballet: unveiling the dynamics of metal bioavailability in sediments following resuspension and reequilibration. *Environ. Sci. Technol.* **2024**, *58* (51), 22755–22765.

(61) Jusup, M.; Sousa, T.; Domingos, T.; Labinac, V.; Marn, N.; Wang, Z.; Klanjšček, T. Physics of metabolic organization. *Phys. Life Rev.* **2017**, *20*, 1–39.

(62) Kooijman, S. A. L. M.; Metz, J. A. J. On the dynamics of chemically stressed populations: The deduction of population consequences from effects on individuals. *Ecotoxicol. Environ. Saf.* **1984**, *8* (3), 254–274.

(63) Jager, T. Revisiting simplified DEBtox models for analysing ecotoxicity data. *Ecol. Model.* **2020**, *416*, 108904.

(64) Jager, T.; Zimmer, E. I. Simplified dynamic energy budget model for analysing ecotoxicity data. *Ecol. Model.* **2012**, *225*, 74–81.